CrystEngComm

Accepted Manuscript

ROYAL SOCIETY OF CHEMISTRY

www.rsc.org/crystengcomm

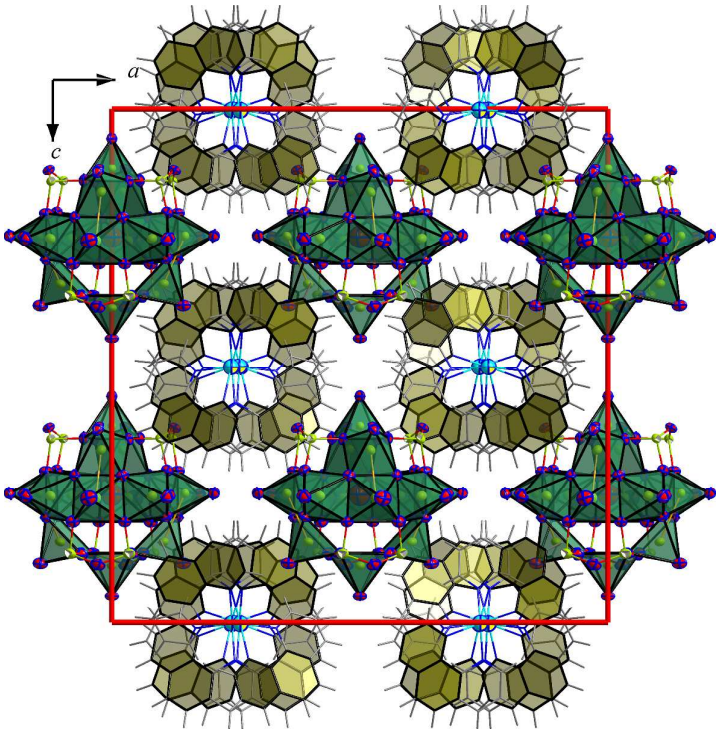

Three new arsenic-vanadium compounds have been prepared hydrothermally and characterized. We discussed the influence of transition metal complexes on the crystal structures. Also we analyzed the catalytic properties of the compounds and discussed the influence of the crystal structures of transition metal complexes to the catalytic properties.

Journal Name

Dynamic Article Links ►

Cite this: DOI: 10.1039/c0xx00000x

www.rsc.org/xxxxxx

ARTICLE TYPE

The synthesis and characterizations of three organic-inorganic hybrids based on different transition metal complexes and $\{As_8V_{14}O_{42}(H_2O)\}$ clusters and the influence of structures to their catalytic properties

Hai-Yang Guo,[a] Zhi-Fang Li,[b] De-Chuan Zhao,[a] Yang-Yang Hu,[a] Li-Na Xiao,[a] Xiao-Bing Cui,*[a] and Jing-Qi Guan,*[b] Ji-Qing Xu[a]

Received (in XXX, XXX) Xth XXXXXXXXX 20XX, Accepted Xth XXXXXXXXX 20XX
DOI: 10.1039/b000000x

Three new arsenic-vanadium compounds, $[As_8V_{14}O_{42}(H_2O)][Cu(2,2'\text{-bpy})_2]_4$ (**1**) $[As_8V_{14}O_{42}(H_2O)][Cu(1,10\text{-Phen})_2]_4$ (**2**) and $[As_8V_{14}O_{42}(H_2O)][Ni(Biim)_3]_2{\cdot}6H_2O$ (**3**) (2,2'-bpy=2,2'-bipyridine, 1,10-Phen=1,10-phenanthroline and Biim= 2,2'-Biimidazole), have been prepared hydrothermally and characterized by IR, UV-Vis, XRD, XPS, and single-crystal X-ray diffraction analyses. X-ray crystallographic study showed that compounds **1**-**3** are all based on the cluster anion $[As_8V_{14}O_{42}(H_2O)]^{4-}$. However, the crystal structures of the three are thoroughly different. It is obvious that transition metal complex building blocks are the vital factor for the packing structures of the three. We carefully discussed the influence of transition metal complex building blocks on the crystal structures. Also we analyzed the catalytic properties of the compounds and discussed the influence of the crystal structures of transition metal complexes to the catalytic properties.

Introduction

The chemistry of polyoxometalates continues to attract interest as a result of their realized and potential applications in diverse fields, such as catalysis, analysis, biochemistry, medicine and material science.[1] This class of metal-oxygen clusters is formed by early transition metals of groups V and VI (V, Nb, Ta, Mo and W) in their highest oxidation states (e.g., V^{5+}, W^{6+}).[1a] Although a large number of heteropoly- and isopolyanions have been prepared and isolated from both aqueous and nonaqueous solutions,[1a] the mechanism for the formation of POMs is still elusive, even very complex structures can be synthesized in one-pot reactions by interactions of composing elements without the need of any polyoxoanion precursor species. Therefore, the discovery of new POMs with completely unexpected structures and properties is not uncommon.[2]

In the past few decades, the design and synthesis of organic-inorganic hybrid compounds based on POMs have become a hotspot due to their novel structures and unusual properties.[3] An important subclass of polyoxometalates is the family of arsenic-vanadium clusters with arsenic and vanadium in low oxidation states. The arsenic-vanadium clusters can be mainly categorized into two different groups based on the number of arsenic and vanadium atoms: As_8V_{14} and As_6V_{15} clusters. The first case is represented by anions $[As_8V_{14}O_{42}(X)]^{n-}$ ($X = SO_3^{2-}$ or SO_4^{2-}, n=6; X=H_2O, n=4),[4] and the second group can be exemplified by compounds $K_6[As_6V_{15}O_{42}(H_2O)]\cdot 8H_2O$ [5] and $K_6[As_6V_{15}O_{42}(H_2O)]\cdot 6H_2O$.[6] Although some organic-inorganic hybrid compounds based on As-V-O POMs have been obtained to date, such as $[NHEt_3]_2[NH_2Me_2][As_8V_{12}O_{40}(HCO_2)]\cdot 2H_2O$,[7] $[NBu_4]_4[As_8V_6O_{26}]$,[8] $[Co(2,2'\text{-bpy})_3]_2[As_8V_{14}O_{42}(H_2O)]\cdot 3H_2O$ and $[2,2'\text{-bpy}][Ni(2,2'\text{-bpy})_3]_2[As_8V_{14}O_{42}(H_2O)]\cdot 3H_2O$,[9] the chemistry of hybrids based on As-V-O POMs is less developed. Our group has focused on the exploitation of As-V-O POMs for years.[10] And recently we began to choose $[As_8V_{14}O_{42}(H_2O)]^{4-}$ clusters as building blocks to form different organic-inorganic hybrid compounds. It is easy to see the influence of transition metal complex building blocks on the crystal structures.

In this paper, we report hydrothermal syntheses and structural characterizations of three new compounds $[As_8V_{14}O_{42}(H_2O)][Cu(2,2'\text{-bpy})_2]_4$ (**1**) $[As_8V_{14}O_{42}(H_2O)][Cu(1,10\text{-Phen})_2]_4$ (**2**) and $[As_8V_{14}O_{42}(H_2O)][Ni(Biim)_3]_2\cdot 2H_2O$ (**3**). Compounds **1** and **2** are based on the same $[As_8V_{14}O_{42}(H_2O)]^{4-}$ POM and very similar transition metal complexes (TMCs). However, the resulting supramolecular structures based on POMs and the two similar TMCs are thoroughly different. By contrast, compound **3** is a new compound based on $[As_8V_{14}O_{42}(H_2O)]^{4-}$ anions and $[Ni(Biim)_3]^{2+}$ TMCs, which also exhibits a supramolecular structure. It is well-known that oxidation of olefins to their corresponding epoxides is one of the important reactions in the production of a wide variety of fine chemicals and chemical intermediates.[11] Organic-inorganic hybrids based on POMs are good candidates as a new type of POM-based catalysts. Recently, the oxidation of styrene with Keggin-POM-based hybrids, the oxidation of some olefins with Anderson-POM-based hybrids and the oxidation of cyclooctene with oxtamolybdate-bsaed hybrids have been reported.[12] Herein, we report the epoxidation of both styrene and cyclooctene with the three hybrids based on $[As_8V_{14}O_{42}(H_2O)]^{4-}$ polyanions in this paper.

Experimental

All chemicals used during the course of this work were of reagent grade and used as received from commercial sources without further purification. IR spectra were obtained on a Perkin-Elmer spectrophotometer from 200-4000cm^{-1} with pressed KBr pellets. XPS measurements were performed on single crystals with an ESCALAB MARK II apparatus using a Mg-Kα X-ray radiation as the excitation source (1253.6eV). Elemental analyses of As, V, Cu and Ni were determined by inductively coupled plasma (ICP) analyses on a Perkin-Elmer Optima 3300DV ICP spectrometer. UV-Vis spectra of dimethyl sulfoxide saturated solutions of compounds **1-3** were recorded on a Shimadzu UV-3100 spectrophotometer. Small-angle X-ray diffraction (XRD) patterns were obtained on a Siemens D5005 diffractometer using a Cu Kα radiation.

Synthesis of $[As_8V_{14}O_{42}(H_2O)][Cu(2,2'\text{-bpy})_2]_4$ (1)

Compound **1** was synthesized hydrothermally by reacting of V_2O_5 (0.296g, 1.63mmol), $H_2C_2O_4\cdot H_2O$ (0.525g, 4.16mmol), $NaAsO_2$ (0.470g, 3.62mmol), $Cu(Ac)_2$ (0.186g, 0.93mmol), 2,2'-bpy (0.052g, 0.33mmol) and H_2O (10ml) was stirred for 2h, and then was sealed in a Teflon-lined stainless bomb and heated at 160℃for 5 days. The pH of the mixture was necessarily adjusted to 4 with $NH_3\cdot H_2O$ solution. The resulting black columnar crystals of **1** were filtered off, washed with water, and air-dried at room temperature (ca, 15.0% yield based on V). Calcd. For $C_{80}H_{66}As_8V_{14}Cu_4O_{43}N_{16}$: As, 17.10; Cu, 7.25; V, 20.34; C, 27.41; H, 1.90; N, 6.39%; Found: As, 16.95; Cu, 7.01; V, 20.18; C, 27.33; H, 1.26; N, 6.29. IR (cm^{-1}): 3551, 3440, 3062, 1624, 1593, 1570, 1466, 1440, 1311, 1277, 1246, 1158, 995, 898, 824, 762, 712, 630, 556, 462. Compound **1** can also be prepared by only adjusting pH to 5 and 6, however, the crystal quality is not as good as that prepared at pH of 4. We also applied the same procedure except that 2,2'-bpy (0.052g, 0.33mmol) was replaced by 1,10-Phen (0.065g, 0.33mmol), and we only got some unidentified amorphous materials.

Synthesis of $[As_8V_{14}O_{42}(H_2O)][Cu(1,10\text{-Phen})_2]_4$ (2)

Table 1. Crystal data and structural refinements for compounds **1** - **3**.

	Compound **1**	Compound **2**	Compound **3**
Empirical formula	$C_{80}H_{66}As_8Cu_4N_{16}O_{43}V_{14}$	$C_{96}H_{66}As_8Cu_4N_{16}O_{43}V_{14}$	$C_{36}H_{50}As_8N_{24}Ni_2O_{49}V_{14}$
Formula weight	3506.17	3698.33	3032.94
Crystal system	tetragonal	orthorhombic	tetragonal
space group	I4(1)/a	Aba2	I4(1)/a
a (Å)	28.369(4)	26.4776(12)	15.118(2)
b (Å)	28.369(4)	16.8267(11)	15.118(2)
c (Å)	14.436(3)	27.5248(11)	38.962(8)
α (°)	90	90	90
β (°)	90	90	90
γ (°)	90	90	90
Volume ($Å^3$)	11618(3)	12263(1)	8905(2)
Z	4	4	4
D_C ($Mg·m^{-3}$)	2.004	2.003	2.262
μ (mm^{-1})	4.130	3.919	4.861
F(000)	6816	7200	5872
θ for data collection	3.00 to 27.48	2.09 to 27.13	3.06 to 27.47
Reflections collected	54802	36617	42022
Reflections unique	6639	12718	5056
R(int)	0.0963	0.0517	0.0465
Completeness to θ	99.5	99.7	99.2
parameters	373	819	302
GOF on F^2	1.004	0.998	1.036
R^a [I>2σ(I)]	R_1 = 0.0654	R_1 = 0.0558	R_1 = 0.0379
R^b (all data)	ωR_2 = 0.2244	ωR_2 = 0.1519	ωR_2 = 0.1084

[a] $R_1 = \sum||F_0|-|F_c||/\sum|F_0|$. [b] $\omega R_2 = \{\sum [w (F_0^2-F_c^2)^2]/\sum[w(F_0^2)^2]\}^{1/2}$.

Compound **2** can be synthesized hydrothermally by reacting V_2O_5 (0.222g, 1.2mmol), $H_2C_2O_4·H_2O$ (0.291g, 2.3mmol), $NaAsO_2$ (0.147g, 1.2mmol), $CuCl_2·2H_2O$ (0.190g, 1.0mmol), 1,10-Phen (0.072g, 0.35mmol), im (0.057g, 0.8mmol) and distilled water (10 ml) in a Teflon-lined autoclave. The pH of the mixture was necessarily adjusted to 4 with $NH_3·H_2O$ solution. The mixture was heated under autogenous pressure at 160℃ for 5 days and then left to cool to room temperature. Crystals could be isolated at 25% yield (based on V). Anal. Calcd for $C_{96}H_{66}As_8V_{14}Cu_4O_{43}N_{16}$: As, 16.21; Cu, 6.87; V, 6.06; C, 31.18; H, 1.80; N, 6.06%. Found: As, 16.07; Cu, 7.01; V. 6.14; C, 31.10; H. 1.36; N, 6.00. IR (cm^{-1}): 3441, 3057, 1620, 1507, 1422, 1220, 1144, 1000, 849, 821, 767, 715, 632, 556, 473. The same procedure except that 1,10-Phen (0.072g, 0.35mmol) was replaced by 2,2-bpy (0.054g, 0.35mmol) was carried out, and we only got some dark red solution. After the solution was evaporated slowly, only some unidentified amorphous materials were left.

Compound **2** can also be synthesized hydrothermally by reacting V_2O_5 (0.500g, 2.7mmol), $H_2C_2O_4·H_2O$ (0.500g, 4.0mmol), $NaAsO_2$ (0.203g, 1.6mmol), $CuSO_4·5H_2O$ (0.213g, 0.85mmol), 2,2'-bpy (0.051g, 0.3mmol), 1,10-Phen (0.072g, 0.4mmol) and distilled water (10 ml) in a Teflon-lined autoclave. The mixture was necessarily adjusted to pH 5 with $NH_3·H_2O$ solution. The pH of the mixture was heated under autogenous pressure at 160℃ for 5 days. The attempts to isolate compound **2** by removal of both Im or 2,2'-bpy are not successful.

The crystal quality of both compounds **1** and **2** is better when pH is 4. We have done the synthesis for As-V-O POMs for years, [10] our previous work has demonstrated that As_8V_{14} is easy to be synthesized under weakly acidic conditions, and a Cu coordination complex based on aromatic nitrogen-containing ligands is also easy to be prepared under weakly acid conditions too. Thus, compounds **1** and **2** are synthesized under pH values of 4-6 and 4-5, respectively, and the optimal pH value is 4.

The molar ratio of V_2O_5 to $NaAsO_2$ for compound **1** is about 1:2, and the molar ratios of V_2O_5 to $NaAsO_2$ for compound **2** are 1:1 and about 2:1. The molar ratio selected is not very sensitive to As_8V_{14} in the final product.

Synthesis of $[As_8V_{14}O_{42}(H_2O)][Ni(Biim)_3]_2·6H_2O$ （3）

Compound **3** was synthesized hydrothermally by reacting $NaAsO_2$(0.331g, 2.5mmol), NH_4VO_3 (0.201g, 2mmol), $H_2C_2O_4·H_2O$ (0.364g, 3mmol), $NiCl_2·6H_2O$ (0.285g, 1mmol), Biim (0.051g, 0.4mmol), 4,4'-bpy (0.055g, 0.4mmol) and distilled water (10 ml) in a Teflon lined autoclave. The pH of the reaction mixture was 3. The mixture was heated under autogenous pressure at 160°C for 5 days and then left to cool to room temperature. Crystals could be isolated at 42% yield (based on V). Anal. Calcd for $C_{36}H_{50}As_8V_{14}Ni_2O_{49}N_{24}$: As, 19.76; Ni, 3.87; V, 23.52; C, 14.26; H, 1.66; N, 11.08%. Found: As, 19.24; Ni, 3.97; V, 24.09; C, 14.11; H, 1.43; N, 11.35%. IR (cm^{-1}): 3490, 3124, 2999, 2921, 1624, 1527, 1499, 1425, 1319, 1239, 1181, 1127, 1104, 999, 956, 825, 752, 715, 556.

X-ray crystallography

Crystal structures of compounds **1-3** were determined by single-crystal X-ray diffraction. The intensity data of compounds **1-3** were collected on a Bruker Smart-CCD diffractometer equipped with a Mo Kα radiation (λ = 0.71073Å) at 293(2) K. No crystal showed evidence of crystal decay during data collections. The three structures were solved by direct methods and refined using full-matrix least squares on F^2 with the SHELXTL-97 crystallographic software package. In final refinements, all non-

hydrogen atoms were refined anisotropically. The hydrogen atoms of 1,10-Phen, bpy and Biim ligands were placed in calculated positions and included in the structure factor calculations but not refined, while hydrogen atoms of water molecules were not added. CCDC number: 973724 for compound **1**, 973725 for compound **2**, and 973726 for compound **3**. These data can be obtained free of charge via www.ccdc.cam.ac.uk/conts/retrieving.html (or from the Cambridge Crystallographic Data Centre, 12, Union Road, Cambridge CB2 1EZ, UK; Fax: (+44) 1223-336-033; or deposit@ccdc.cam.ac.uk).

Results and discussion

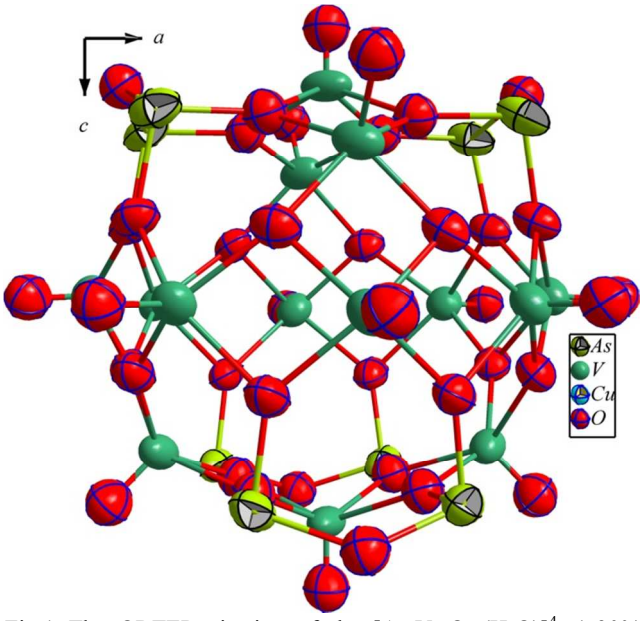

Fig.1 The ORTEP viewing of the $[As_8V_{14}O_{42}(H_2O)]^{4-}$ (30% probability ellipsoids).

Crystal structure of compound 1. The asymmetric unit of compound **1** consists of one fourth of $[As_8V_{14}O_{42}(H_2O)]^{4-}$ and a $[Cu(2,2'\text{-bpy})_2]^{+}$ transition metal complex. The polyanion is almost identical to the cluster $[As_8V_{14}O_{42}(0.5H_2O)]^{4-}$ [4a] with only slight differences in bond lengths and angles and a water molecule replacing the half one. As shown in Fig. 1, the vanadium atoms of $[As_8V_{14}O_{42}(H_2O)]^{4-}$ adopt a pyramidal geometry, with four μ_3 oxygen atoms forming the base plane with V-O distances in the range of 1.912(5)-2.009(6)Å and a terminal oxygen occupying the apical position with V-O distances ranging from 1.552(9)-1.594(6)Å. Each arsenic atom is coordinated by three μ_3 oxygen atoms with As-O distances of 1.750(5)-1.779(6)Å, exhibiting a trigonal pyramidal geometry. Based on the results of bond-valence sum calculations,[13] all the V atoms are in the +4 oxidation state, and the As atoms have a +3 oxidation state. Thus, the polyhedron of As^{III} can be described as a ψ-AsO_3 tetrahedron with one corner of the tetrahedron occupied by the lone pair of electrons.

The packing motif of POMs of compound **1** is shown in Fig.2. Red lines represent the edges of the cell of compound **1**. The parallel upper and lower faces of the cell are shown in green, while the middle plane in the cell is shown in pink. There are two POMs with their centers located on the upper face with the distance of the two of 14.637(2)Å, whereas there are two POMs with their centers located on the middle plane with the distance of the two of 17.845(2)Å. It should be noted that the arrangement of the two POMs of the lower face is just identical to the ones of the upper face. That is to say, the two POMs of upper face plus the two POMs of the middle plane form the repeating unit of the packing structure of POMs.

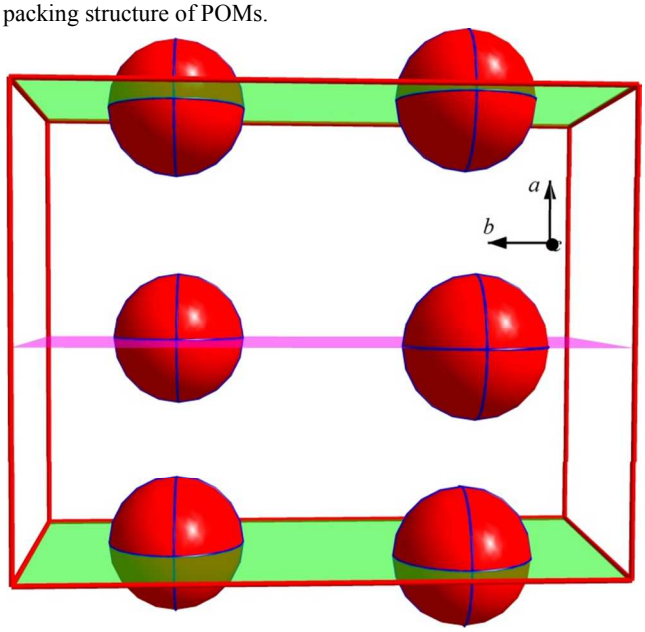

Fig. 2 The topological view of the packing strucutre of POMs in compound **1**. The big red balls represent the POMs in compound **1**.

The Cu^{I} ion of the TMC is coordinated in a tetrahedral configuration by four N atoms from two 2, 2-bpy ligands with Cu-N distances in the range of 1.98(1)-2.00(1)Å, indicating that the oxidation state of the copper centre is +1. The +1 oxidation state of the copper ion is also comfirmed by the BVS calculation (1.14 for Cu(1)). [13] Each TMC contains four pyridine rings. However, the crystal analysis does not suggest the existence of intermolecular or intramolecular $\pi\cdots\pi$ interactions between pyridine rings of any copper TMCs (confirmed by PLATON software).[14] The reason comes from that the angles between the two pyridine rings of each 2,2'-bpy ligand are 8.302º and 13.162º, indicating that the neighboring 2,2'-bpy ligands are hard to be parallel to each other and then $\pi\cdots\pi$ interact with each other.

The crystal analysis strongly suggests the existence of C-H···O interactions between carbon atoms of TMCs and oxygen atoms of POMs. Each TMC is hydrogen-bonded to two neighbouring POMs via C(8)-H(8)···O(6a, 1.5-x, 0.5-y, 0.5-z), C(17)-H(17)···O(9) and C(13)-H(13)···O(5) with C···O distances in the range of 2.9971(4)-3.1850(3)Å, while each POM is linked to eight Cu(1) TMCs via above-mentioned hydrogen bonds and their symmetry equivalent ones. Through C-H···O interactions, TMCs and POMs are connected into a 3-D supramolecular layer structure.

The packing structure of TMCs in compound **1** is directed by the templating effect of POMs through C-H···O interactions into a novel 1-D supramolecular column, as shown in Fig. s1. The repeating unit of the supramolecular column is comprised of four $[Cu(1)(2,2\text{-bpy})_2]^{+}$ complexes. When the viewing direction is along the *c* axis, the cross section of the supramolecular column

exhibits a square planar motif, when the viewing direction is along the *a* axis, we can see that the copper ions are arranged into a supramolecular 1-D zigzag chain structure (Fig. 3).

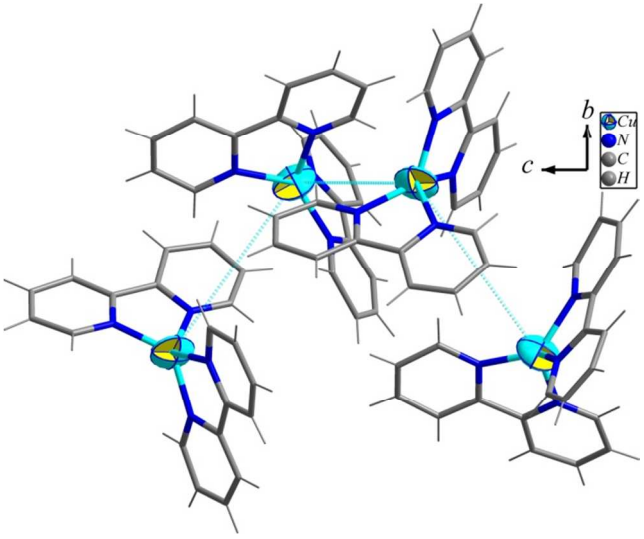

Fig. 3 The supramolecular 1-D zigzag chain structure formed by the $[Cu(1)(2,2\text{-bpy})_2]^+$ complexes along the a axis.

Crystal structure of compound 2. The asymmetric unit of compound **2** is composed of half a $[As_8V_{14}O_{42}(H_2O)]^{4-}$ and two $[Cu(1,10\text{-Phen})_2]^+$ TMCs. It should be noted that compounds **1** and **2** have very similar compositions. They are based on the identical polyanion and very similar TMCs. However, the structures of the two are thoroughly different. Compound **1** crystallizes in tetragonal space group I4(1)/a, whereas compound **2** crystallizes in orthorhombic space group Aba2.

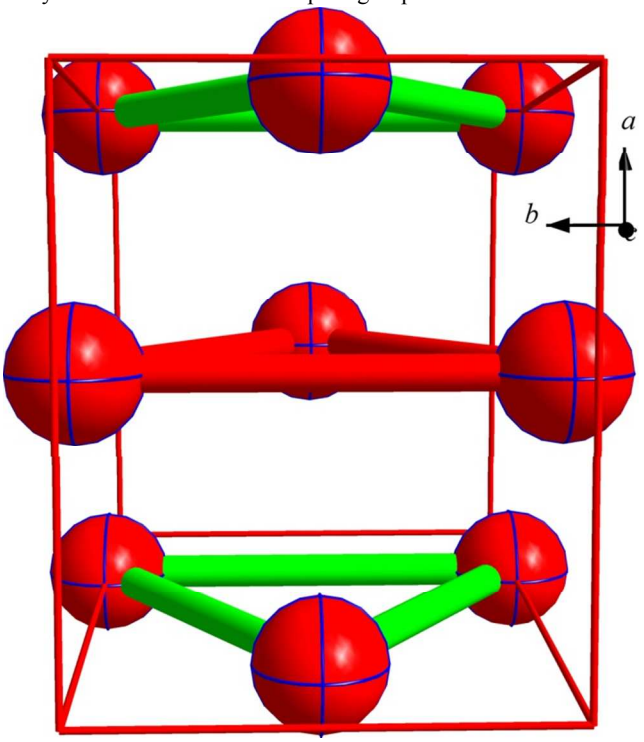

Fig. 4 The topological view of the packing structure of POMs in compound **2**. The big red balls represent the POMs in compound **2**.

The packing motif of POMs of compound **2** is shown in Fig.4. Red lines represent the edges of the cell of compound **2**. There are three POMs with their centers located on the upper face of the cell. The three POMs are arranged in an isosceles triangle motif. The two equal sides of the triangle are 16.1305(3)Å in length, while the base is 16.8267(1)Å in length. It should be noted that the triangle on the lower face of the cell is identical to that of the upper face. There are also three POMs with their centers located on the middle plane in the cell arranged in an isosceles triangle motif, too. The isosceles triangle has the same side and base lengths to those of triangles of the upper and lower faces. However, the apex of the isosceles triangle of the middle plane points in the $-c$ direction, whereas the apexes of the isosceles triangles of the upper and lower faces point in the $+c$ direction. It should be noted that the isosceles triangle of the middle plane and the upper face form the repeating unit of the packing structure of the POMs.

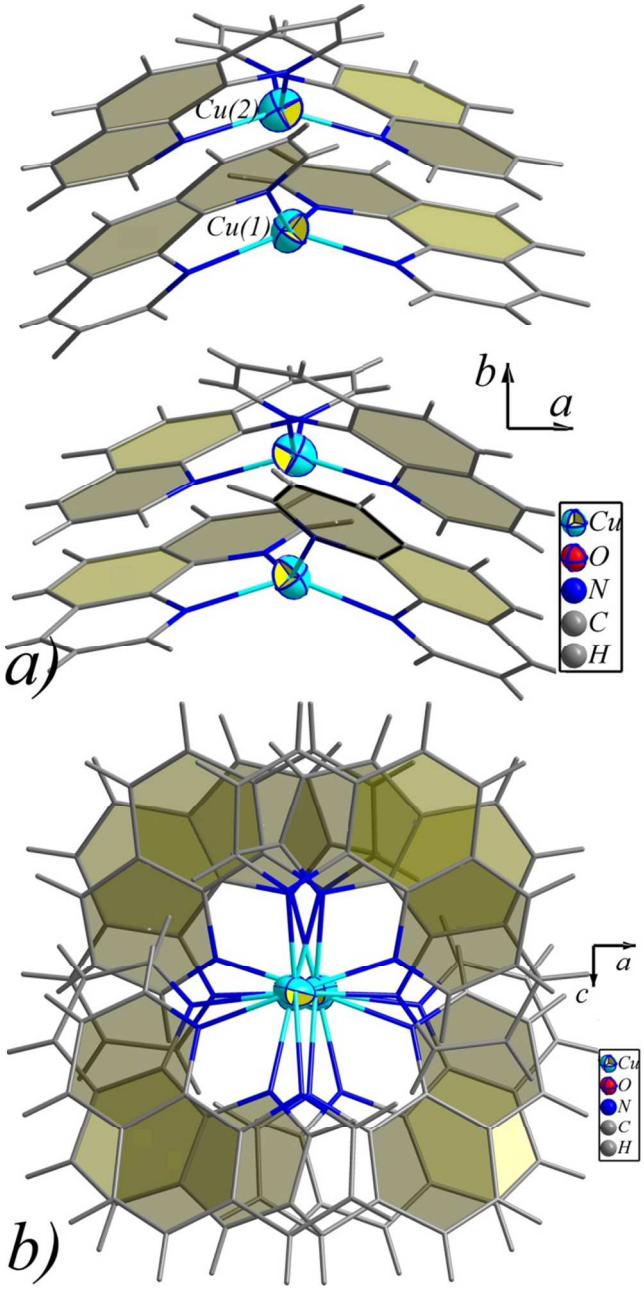

Fig. 5 The side-view (a) and the upper-view (b) of of the supramolecular column formed by copper TMCs.

There are two crystallographically independent copper TMCs in compound **2**. Each of which adopts a tetrahedral geometry, defined by four nitrogen atoms from two 1,10-Phen ligands with Cu-N distances ranging from 2.019(9) to 2.083(9)Å. The crystal analysis strongly suggests the existence of intermolecular π···π interactions between aromatic rings of neighboring copper TMCs. As shown in Fig. 5, the aromatic rings of N(3) and N(2) 1,10-Phen from Cu(1) TMC are respectively linked to the aromatic rings of N(8) and N(6) 1,10-Phen from Cu(2) TMC via intermolecular π···π interactions with face to face stacking distances of about 3.50Å. Through these synergistic intermolecular π···π interactions, Cu(1) and Cu(2) TMCs are connected into a dimer with the Cu-Cu distance of 4.0713(3)Å. It should be noted there are no π···π interactions between any two neighboring dimers. However, it is very interesting that the dimers are arranged along the *b* axis into a 1-D supramolecular column structure as shown in Fig. 5. It should be noted that Cu(1) and Cu(2) copper ions are almost located at the center of the supramolecular column into an almost straight chain with the 1,10-Phen ligands almost fully-wrapping the copper chain.

The crystal analysis also suggests that each dimer is hydrogen bonded to two neighbouring POMs via C(25)-H(25)···O(21a, 0.5+x, 1.5-y, z), C(10)-H(10)···O(21) and C(42)-H(42)···O(7a, 0.5-x, y, 0.5+z) with C···O distances of 2.9699(1)-3.1856(1)Å, whereas each POM is hydrogen bonded to four dimers via above mentioned C-H···O hydrogen bonds and their symmetry equivalents. Throng the C-H···O hydrogen bonds, POMs and dimers are connected into a 3-D supramolecular structure.

Crystal structure of compound 3. The asymmetric unit of compound **3** is composed of one fourth of a $[As_8V_{14}O_{42}(H_2O)]^{4-}$ and half a $[Ni(Biim)_3]^+$ TMC. The TMC in compound **3** is thoroughly different from the TMCs in compounds **1** and **2**. Therefore, the packing structure of compound **3** is thoroughly different from those in compounds **1** and **2**.

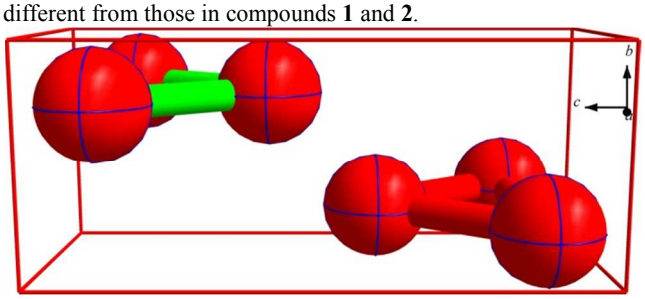

Fig. 6 The topological view of the packing structure of POMs in compound **1**. The big red balls represent the POMs in compound **3**.

The packing motif of POMs of compound **3** is shown in Fig.6, red lines represent the edges of a cell of compound **3**. There are three POMs with their centers arranged in an isosceles triangle motif too. The two equal sides of the triangle are 12.330(2)Å in length, while the base is 15.118(2)Å in length. It should be noted that there are two such triangles in the cell with their apexes pointing in opposite directions. As shown in Fig. 6, the planes through the POM centers of the two triangles are parallel to each other and also parallel to the upper or lower faces of the cell.

The nickel center of the $[Ni(Biim)_3]^+$ TMC is coordinated by six nitrogen atoms from three Biim ligands with Ni-N distances in the range of 2.057(4)-2.136(4)Å (Fig. s2). The crystal analysis also does not suggest the existence of intermolecular or intramolecular π···π interactions between imidazole rings of any copper TMCs (confirmed by PLATON software).

The crystal analysis reveals that each TMC is hydrogen bonded to two POMs via C(5)-H(5)···O(2a, 0.25+x, -0.25-y, 0.25+z) and its symmetry equivalent, respectively, while each POM interacts with four Ni(1) TMCs via above mentioned hydrogen bond and three of its symmetry equivalents. The C···O distance is 3.1857(4)Å. Except for the C-H···O interactions, there also exist O-H···O interactions between oxygen atoms of water molecules and oxygen atoms of POM anions. Ow(1) is hydrogen bonded to O(2) and its symmetry equivalent from two neighboring POMs with O···O distance of 2.7555(3)Å, meaning that the Ow(1) acting as a bridge linking two POMs. Ow1 is also hydrogen bonded to two Ow(2) (Ow(2a, -0.5+x, 1+y, 0.5-z) and its symmetry equivalent) with O···O distances of 2.9572(4)Å, forming a tri-nuclear water cluster. The hydrogen bonds are also formed between Ow(2a, -0.5+x, 1+y, 0.5-z) and O(9a, -0.25+y, -0.25-x, 0.25-z) and O(10a, -0.25-y, 0.25+x, 0.25+z) with O···O distances of 2.8474(4)-2.9678(4)Å. Through these complex C-H···O and O-H···O interactions, POMs and TMCs are connected into a novel 3-D supramolecular structure.

Characterizations

In the IR spectrum of compound **1** (Fig. s3), The band at 995 cm^{-1} is associated with the terminal V=O stretch $\upsilon(V{=}O_t)$ vibration, and strong features at 824cm^{-1} and 712cm^{-1} are ascribed to υ(O-V-O) vibrations. The pattern of bands in the region characteristic of $\upsilon(V{=}O_t)$ indicates the presence of V^{IV} sites: clusters which contain exclusively V^{IV} generally possess $\upsilon(V{=}O_t)$ bands in the range of 970-1000cm^{-1}, while bands in the region 940-960cm^{-1} are characteristic of V^V. The observation of a strong absorbance in the 970-1000cm^{-1} region provides a useful diagnostic for the presence of V^{IV} centers. The band at 762cm^{-1} corresponds to the υ(As-O) vibration. Bands in the 1158-1624cm^{-1} region of the IR spectrum of compound **1** are due to vibrations of 2,2'-bpy ligands in **1**.

Both compounds **2** and **3** are based on $[As_8V_{14}O_{42}(H_2O)]^{4-}$ anions. Thus, they display similar IR spectra to that of compound **1** with slight differences. The IR spectra of compounds **2** and **3** (Fig. s3) show the characteristic peaks at 1000cm^{-1} and 999cm^{-1} corresponding to the $\upsilon(V{=}O_t)$ vibration, respectively. 821cm^{-1}, 715 cm^{-1} for compound **2** and 825cm^{-1}, 715cm^{-1} for compound **3** are due to υ(O-V-O) vibrations, respectively, while the peaks at 767cm^{-1} for compound **2** and 752cm^{-1} for compound **3** can be ascribed to the υ(As-O) vibration, respectively. In addition, bands in the 1124-1620cm^{-1} region of the IR spectrum of compound **2** are due to vibrations of 1,10-Phen ligands and bands in the 1104-1624cm^{-1} region of the IR spectrum of compound **3** are due to vibrations of Biim ligands.

Fig. s4 shows the XPS spectrum of vanadium atoms in compound **1** with two peaks at 516.1eV and 523.9eV ascribed to V^{4+} 2p3/2 and V^{4+} 2p1/2. The XPS spectra of vanadium atoms in compounds **2** and **3** are similar to that of compound **1**, which exhibit two peaks at 516.2eV, 524.3eV and 516.2eV, 523.9eV, respectively, we assigned these to sites of V^{4+} in compounds **2** and **3**.

The XPS spectrum of arsenic in compound **1** is shown in Fig. s4. A single As 3d photoelectron peak occurs at 44.7eV corresponding to the characteristic peak position of As(III). The XPS spectra of arsenic in compounds **2** and **3** show similar peaks at 44.7eV and 44.5eV, respectively, ascribed to the As(III) in compounds **2** and **3**. The XPS estimations obtained on the valence state values are in reasonable agreement with those calculated from bond valence sum calculations of compounds **1-3**.

The XPS spectra of copper in compounds **1** and **2** were recorded with peaks at 933.5eV, 953.2eV and 933.0eV, 953.1eV, respectively, corrresponding to the +1 oxdiation state of copper ions in compounds **1** and **2 (**Fig. s4**)**.

The powder X-ray diffraction patterns for compounds **1-3** are all in good agreement with the ones simulated based on the data of the single-crystal structures, respectively, indicating the purity of the as-synthesized products (Fig. s5). The differences in reflection intensity are probably due to preferential orientations in the powder samples of compounds **1-3**.

The UV-Vis spectra of compounds **1-3,** in the range of 280-400nm, are presented in Fig. s6. The UV-Vis spectrum of compound **1** displays an intense absorption peak centred at about 308nm assigned to an O→V charge transfer. The UV-Vis spectra of compounds **2** and **3** exhibit similar intense absorption peaks to that of compound **1** at 299nm and 296nm, 305nm, respectively, these peaks are attributed to charge transfer bands of O→V in compounds **2** and **3**, respectively.

Table 1 Catalytic activity and product distribution

Entry	Catalysts	Styrene conversion (%)	Product selectivity (%)	
			so	bzdh
1	No catalyst	≈ 0		
2	Compound **1**	75.8	66.5	33.5
3	Compound **2**	51.9	74.7	25.3
4	Compound **3**	83.1	23.1	76.9
5	Compound **4**	48.1	51.5	48.5

so = styrene oxide; bzdh = benzaldehyde. Compound **4:** $[As_8V_{14}O_{42}(H_2O)][Cd(1,10\text{-Phen})_3]_2$. [15] Compound **4** was introduced to compare the influence of different metal ions to their catalysis properties.

The epoxidation of styrene to styrene oxide with aqueous tertbutyl hydroperoxide (TBHP) using compounds **1**, **2**, **3** or **4** as catalyst was carried out in a batch reactor. In a typical run, the catalyst (**1** (10mg, 2.9μmol), **2** (10mg, 2.7μmol), **3** (10mg, 3.3μmol) or **4** (10mg, 3.0μmol)), 1 mmol of styrene and 1 ml of CH_3CN were added to a 10 ml two-neck flask equipped with a stirrer and a reflux condenser. The mixture was heated to 80°C and then 2 mmol of TBHP was injected into the solution to start the reaction. The liquid organic products were quantified by using a gas chromatograph (Shimadzu, GC-8A) equipped with a flame detector and an HP-5 capillary column and identified by a comparison with authentic samples and GC-MS coupling. The activity of the reaction system to oxidize styrene to styrene oxide in the absence of the catalysts was determined. The result showed that no conversion of the styrene was detected after 8 h.

Table 1 shows the reaction results of TBHP oxidation of styrene over various catalysts at 80ºC. As expected, all the catalysts are active for the TBHP oxidation of styrene. Compound **1** catalyst shows the activity with 75.8% conversion and 66.5% selectivity to styrene oxide after 8h. Nevertheless, compound **2** shows the low activity with 51.9% conversion of styrene and 74.7% selectivity to styrene oxide. It is obvious that compound **3** catalyst shows a higher conversion of 83.1% but much lower selectivity (23.1%) to styrene oxide in epoxidation of styrene using TBHP. Compound **4** shows the lowest conversion (48.1%) of the four with 51.5% selectivity to styrene oxide.

The catalytic results for TBHP epoxidation of styrene over the catalysts **1**, **2**, **3** and **4** indicate that the catalytic property of compound **3** is different from those of the other three. In the cases of compounds **1**, **2** and **4**, styrene was oxidized to styrene oxide and benzaldehyde with styrene oxide as the major product. In the cased of compound **3**, benzaldehyde becomes the major epoxidation product. The four compounds have the same $[As_8V_{14}O_{42}(H_2O)]^{4-}$ cluster unit, we thus speculate that the difference comes from the transition metal element; both compounds **1** and **2** contain the copper ion. The two thus shows comparable conversion and selectivity. Compounds **3** and **4** contain nickel and cadmium metal ions, thus the conversion and selectivity to styrene oxide are low.

Table 2 Olefin epoxidation catalytic activity

Entry	Catalyst	Cyclooctene conversion (%)	Product selectivity (%)
1	No catalyst	≈ 0	
2	Compound **1**	65.45	100
3	Compound **2**	33.00	100
4	Compound **3**	48.02	100
5	Compound **4**	46.57	100

The conventional organic oxidants (TBHP) produce copious amounts of environmentally undesirable waste.[16] From the sustainable and green chemistry point of view, the use of molecular oxygen or H_2O_2 for the oxidation of olefins is a very attractive and desirable idea.[17] Therefore, H_2O_2 was used as the oxidant for the epoxidation of cyclooctene to cyclooctene oxide.

Epoxidation of cyclooctene to cyclooctene oxide with aqueous H_2O_2 solution using compounds **1**, **2**, **3** or **4** as catalyst was carried out in a batch reactor. In a typical run, the catalyst (**1** (10mg, 2.9μmol), **2** (10mg, 2.7μmol), **3** (10mg, 3.3μmol) or **4** (10mg, 3.0μmol)), 2ml acetonitrile, and 1mmol of cyclooctene were added to a 10 ml two-neck flask equipped with a stirrer and a reflux condenser. The mixture was heated to 80 °C and then 2 mmol of H_2O_2 was injected into the solution to start the reaction. The liquid organic products were quantified by using a gas chromatograph (Shimadzu, GC-8A) equipped with a flame detector and an HP-5 capillary column and identified by a comparison with authentic samples and GC-MS coupling. The activity of the reaction system to oxidize cyclooctene to cyclooctene oxide in the absence of the catalysts was determined. The result showed that no conversion of the cyclooctene was detected after 9h.

The oxidation of cyclooctene using H_2O_2 as oxidant in the presence of compounds **1-4** yields cyclooctene oxide as the only product. As expected, all the catalysts are active for the H_2O_2 oxidation of cyclooctene. Table 2 shows the conversion values for the products in the oxidation experiments. Compound **1** shows the activity with 65.45% conversion to cyclooctene oxide. Compounds **3** and **4** respectively show lower activities with

48.02% and 46.57% conversions to cyclooctene oxide. By contrast, compound **2** shows the lowest activity with 33.00% conversion to cyclooctene oxide.

The catalytic property of compound **2** is strange, so we redo the oxidation experiment except using 1 mmol H_2O_2 replacing 2mmol H_2O_2 in the above-mentioned experiment. The catalytic result indicates that the compound **2** shows a similar activity with 35.49% conversion, which is comparable to the above-mentioned result.

As mentioned above in the discussion of oxidation experiments of styrene, the transition metal element is very important for the catalytic properties of the four compounds. However, in the oxidation experiments of cyclooctene, the catalytic activity of compound **2** becomes the lowest one among the four, whereas the activity of compound **1** still is the highest one among the four, though the two contain the same copper ion. We carefully analyzed the structural difference of the two compounds and found that the difference perhaps comes from the different structures of the transition metal complex of the two compounds.

Transition metal complexes in compound **1** are arranged into a 1-D supramolecular column, as shown in Fig. s1, whereas transition metal complexes in compound **2** are also arranged into a 1-D supramolecular column structure. However, detailed analysis reveals that the column in compound **2** is thoroughly different from that in compound **1**. The copper center of the transition metal complex in compound **1** is almost half-naked. In contrast, the Cu(1) and Cu(2) of the transition metal complexes in compound **2** are almost fully wrapped for the strong π···π interaction and the arrangement of the dimers, as shown in scheme 1. Therefore, the copper ion is hard to be attacked by the styrene from the center of a dimer for the steric hindrance, also the copper ion is not easy to be attacked by the styrene from the center of the two neighboring dimers, because that the two neighboring dimers are also stacked tightly with the Cu-Cu distances of about 4.3642Å. Thus, the activity of compound **2** is lower than that of compound **1** in the oxidation experiments of styrene to styrene oxide. Furthermore, because of the steric hindrance of the cyclooctene is far stronger than that of the styrene, the catalytic activity of compound **2** to cyclooctene oxide then becomes the lowest one among the four.

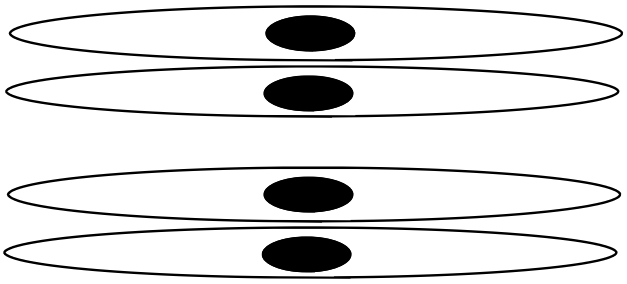

Scheme 1. The schemetic representation of the 1-D supramolecular column structure in compound **2**. The black ball represents the copper ion, and the circle represents the 1,10-Phen ligands.

Conclusions

Three new organic-inorganic hybrid compounds have been synthesized and characterized. The three compounds are all based on the cluster anion $[As_8V_{14}O_{42}(H_2O)]^{4-}$. However, the crystal structures of the three are thoroughly different. It is obvious that transition metal complex building blocks are the vital factor for the packing structures of the three. We carefully discussed the influence of transition metal complex building blocks on the crystal structures. Also we analyzed the catalytic properties of the compounds and discussed the influence of the crystal structure of transition metal complexes to the catalytic properties.

Acknowledgement

This work was supported by National Natural Science Foundation of China under Grant No. 21003056

Notes and references

[a] *College of Chemistry and State Key Laboratory of Inorganic Synthesis and Preparative Chemistry, Jilin University, Changchun, Jilin, 130023. E-mail:cuixb@mail.jlu.edu.cn.*

[b] *College of Chemistry, Jilin University, Changchun 130023, PR China.*

† Electronic Supplementary Information (ESI) available: [details of any supplementary information available should be included here]. See DOI: 10.1039/b000000x/

‡ Footnotes should appear here. These might include comments relevant to but not central to the matter under discussion, limited experimental and spectral data, and crystallographic data.

1. (a)M. T. Pope, *Heteropoly and Isopoly Oxometalates*, Springer-Verlag, Berlin, 1983; (b)M. T. Pope and A. Müller, *Angew. Chem., Int. Ed. Engl.*, 1991, **30**, 34; (c)M. T. Pope and A. Müller, *Polyoxometalate Chemistry: From Topology via Self-Assembly to Applications*, the Netherlands, Kluwer, Dordrecht, 2001.
2. K. Ulrich, N. Saritha, C. S. Ashley, S. D. Naresh, V. T. Johan and S. B. Bassem, *Inorg. Chem.*, 2004, **43**, 144.
3. (a)D. Hagrman, C. Zubieta, D. J. Rose, J. Zubieta and R. C. Haushalter, *Angew. Chem., Int. Ed.*, 1997, **36**, 873; (b)P. J. Hagrman, D. Hagrman and J. Zubieta, *Angew. Chem., Int. Ed.*, 1999, **38**, 2638.
4. (a)G. Huan, M. A. Greaney and A. J. Jacobson, *J. Chem. Soc., Chem. Commun.*, 1991, 260; (b)A. Müller and J. Döing, *Z. Anorg. Allg. Chem.*, 1991, **595**, 251.
5. A. Müller and J. Döing, *Angew. Chem. Int. Ed. Engl.*, 1988, **27**, 1721.
6. G. Y. Yang, L. S. Chen, J. Q. Xu, Y. F. Li, H. R. Sun, Z. W. Pei, Q. Su, Y. H. Lin and Y. Xing, *Acta. Cryst., Sect. C.*, 1998, **54**, 1556.
7. A. Müller, J. Döing and H. Bögge, *J. Chem. Soc., Chem. Commun.*, 1991, 273.
8. E. Dumas, C. Livage, S. Halut and G. Hervé, *Chem. Commun.*, 1996, 243.
9. G. Y. Yang, S. T. Zheng and J. Q. Xu, *J. Clust. Sci.*, 2005, **16**, 1.
10. (a)W. M. Bu, G. Y. Yang, L. Ye, J. Q. Xu and Y. G. Fan, *chem. Lett.*, 2000, 462; (b)X. B. Cui, Y. Q. Sun and G. Y. Yang, *Inorg. Chem. Commun.*, 2003, **6**, 259; (c)X. B. Cui, J. Q. Xu, L. Ding, H. Ding, L. Ye and G. Y. Yang, *J. Mol. Struct.*, 2003, **660**, 131; (d)X. B. Cui, J. Q. Xu, Y. Li, Y. H. Sun, L. Ye and G. Y. Yang, *j. Mol. Struct.*, 2003, **657**, 397; (e)X. B. Cui, J. Q.

Xu, Y. Li, Y. H. Sun and G. Y. Yang, *Eur. J. Inorg. Chem.*, 2004, 1051; (f)X. B. Cui, J. Q. Xu, H. Meng, S. T. Zheng and G. Y. Yang, *Inorg. Chem.*, 2004, **43**, 8005; (g)X. B. Cui, J. Q. Xu, Y. H. Sun, Y. Li, L. Ye and G. Y. Yang, *inorg. Chem. Commun.*, 2004, **7**, 58; (h)X. B. Cui, K. C. Li, L. Ye, Y. Chen, J. Q. Xu, W. J. Duan, H. H. Yu, Z. H. Yi and J. W. Cui, *J. Solid State Chem.*, 2008, **181**, 221; (i)S. Y. Shi, Y. Chen, J. N. Xu, Y. C. Zou, X. B. Cui, Y. Wang, T. G. Wang, J. Q. Xu and Z. M. Gao, *CrstEngComm.*, 2010, **12** 1949.

11. (a)G. A. Barf and R. A. Sheldon, *J. Mol. Catal. A: Chem.*, 1995, **102**, 23-39; (b)B. Notari, *Stud. Surf. Sci. Catal.* , 1991, **60**, 343-352; (c)J. R. Monnier, *Appl. Catal.*, 2001, **A221**, 79-91; (d)M. D. Hughes, Y. J. Xu, P. Jenkins, P. McMorn, P. Landon, D. I. Enache, A. F. Carley, G. A. Attard, G. J. Hutchings, F. King, E. H. Stitt, P. Johnston, K. Griffin and C. J. Kiely, *Nature*, 2005, **437**, 1132-1135.
12. (a)F. Yu, X. J. Kong, Y. Y. Zheng, Y. P. Ren, L. S. Long, R. B. Huang and L. S. Zheng, *Dalton Trans.*, 2009, 9503; (b)F. Yu, P. Q. Zheng, Y. X. Long, Y. P. Ren, X. J. Kong, L. S. Long, Y. Z. Yuan, R. B. Huang and L. S. Zheng, *Eur. J. Inorg. Chem.*, 2010, 4526; (c)D. Dutta, A. D. Jana, M. Debnath, A. Bhaumik, J. Marek and M. Ali, *Dalton Trans.*, 2010, **39**, 11551; (d)J. Du, J. H. Yu, J. Y. Tang, J. Wang, W. X. Zhang, W. R. Thiel and M. J. Jia, *Eur. J. Inorg. Chem.*, 2011, 2361.
13. I. D. Brown, in *Structure and Bonding in Crystals*, eds. M. O'Keefe and A. Navrotsky, Academic Press, New York, 1981, pp. 1–30.
14. A. L. Spek, *PLATON, a multipurpose crystallographic tool*, Utrecht University Utrecht, The Netherlands, 2001.
15. C. L. Wang, G. P. Zhou, Z. B. Zhang, D. R. Zhu and Y. Xu, *J. Coor. Chem.*, 2011, **64**, 1198.
16. S. Khare and R. Chochare, *J. Mol. Catal. A: Chem.*, 2011, **344**, 83-92.
17. Y. Yang, Y. Zhang, S. J. Hao and Q. B. Kan, *Chem. Eng. J.*, 2011, **171**, 1356-1366.